Available online at www.sciencedirect.com
SCIENCE DIRECT®
Thermochimica Acta 408 (2003) 85–96
thermochimica acta
www.elsevier.com/locate/tca

# Sublimation and vaporisation processes of *S*(−) efaroxan hydrochloride

R. Pena [a,*], J.P. Ribet [a], J.L. Maurel [a], L. Valat [a], F. Lacoulonche [b], A. Chauvet [c]

[a] *Département de Chimie, Institut de Recherche Pierre Fabre, 17 avenue Jean Moulin, 81106 Castres, France*
[b] *SA Calytherm, 669 rue Valmont, 34980 St Gely du Fesc, France*
[c] *Laboratoire de Chimie Générale et Minérale, Faculté de Pharmacie, BP 14491, 15 avenue Charles Flahault, 34093 Montpellier, France*

Received 25 November 2002; received in revised form 19 May 2003; accepted 29 May 2003

**Abstract**

Thermogravimetric analysis was used to study the sublimation and vaporisation processes of *S*(−) efaroxan hydrochloride, a potent and highly selective α-2-adrenoreceptor antagonist. The kinetic parameters of the sublimation were investigated by conventional, isothermal thermogravimetric analysis (TGA) and modulated TGA (MTGA). The physico-chemical characterisation of the sublimate was determined by HPLC, elemental analysis, and DSC FTIR spectroscopy. Sublimation followed a zero-order mechanism and the activation energy and pre-exponential factor were calculated.

The sublimation and vaporisation enthalpies were evaluated and used to determine the melting enthalpy, which was seen to be consistent with DSC data. The solubility parameter, which can be used to predict the miscibility of a drug in a polymer, was calculated from vaporisation enthalpy and crystallographic data.

Finally, the Langmuir equation was used to construct the diagram of the sublimation process, $p = f(T)$. The data were fitted using the Antoine equation by a least squares method.


*Keywords:* Kinetic; Sublimation; Vaporisation; TGA; MTGA

## 1. Introduction

Efaroxan hydrochloride is a potent and highly selective α-2-adrenoreceptor antagonist which is currently under investigation for the treatment of neurodegenerative diseases and progressive cognitive deficits, particularly Parkinson's and Alzheimer's diseases [1]. Knowledge of its thermal stability is very important because the development of drug involving thermal and mechanical stresses can lead to drug decomposition.

The thermal and spectral properties have already been established along with the phase diagrams between enantiomers [2,3]. In the initial study, the sublimation of efaroxan hydrochloride was observed by hot stage microscopy between 155 and 250 °C. The melting data were 245.1 ± 0.3 °C and 30.2 ± 0.8 kJ mol$^{-1}$ for optical antipodes.

The purpose of this study was to investigate the nature of the reactions occurring at high temperature, sublimation (phase transition from solid to vapour), vaporisation (phase transition from liquid to vapour) or chemical decomposition.

A kinetic study was conducted by conventional, isothermal thermogravimetric analysis (TGA) and

* Corresponding author. Fax: +33-5-63-714299.
*E-mail address:* richard.pena@pierre-fabre.com (R. Pena).

0040-6031/$ – see front matter © 2003 Elsevier B.V. All rights reserved.
doi:10.1016/S0040-6031(03)00321-6

modulated TGA (MTGA). Friedman and Kissinger methods were used to evaluate the kinetic parameters from non-isothermal experiments while a model fitting method was used in isothermal conditions. MTGA allowed us to predict activation energy as a function of the extent of reaction from one single run. Thermodynamic parameters such as sublimation, vaporisation, melting enthalpies and solubility parameter were also determined.

Finally, the pressure–temperature diagram for the sublimation process was constructed since its knowledge is critical to predict the loss of drug from bulk powders, the thermodynamic stability of polymorphs [4] or the preferential crystallisation conditions.

## 2. Theoretical background

### 2.1. Kinetics

#### 2.1.1. Friedman method

Analysis of the thermogravimetric data is based on the extent of the reaction, $\alpha$

$$\alpha = \frac{W_i - W_t}{W_i - W_f} \tag{1}$$

where $W_t$ is the weight percent of the sample at any time $t$ and $W_i$ and $W_f$ are the initial and final weight percents, respectively.

The non-isothermal experiments were used to determine the dependence of $E_a$ on $\alpha$ by applying the Friedman isoconversional method [5]. The reaction rate is generally described by

$$\frac{d\alpha}{dt} = k(T) f(\alpha) \tag{2}$$

where $f(\alpha)$ depends on the reaction mechanism and $k(T)$ is the rate constant given by the Arrhenius equation (3):

$$k(T) = A' e^{E_a/RT} \tag{3}$$

where $E_a$ is the activation energy, $A$ the pre-exponential factor, $R$ the gas constant and $T$ is the absolute temperature.

For non-isothermal conditions the heating rate, $\beta$, is given by

$$\beta = \frac{dT}{dt} \tag{4}$$

Combining Eqs. (2)–(4) gives

$$\frac{d\alpha}{dT} = \frac{A}{\beta} e^{-E_a/RT} f(\alpha) \tag{5}$$

If we consider logarithms, we obtain the Friedman equation:

$$\ln\left(\beta \frac{d\alpha}{dT}\right) = \ln A + \ln(f(\alpha)) - \frac{E_a}{RT} \tag{6}$$

Plotting $\ln(\beta(d\alpha/dT))$ against $1/T$ give the activation energy for a fixed value of $\alpha$ and variable heating rates.

#### 2.1.2. Kissinger method

Another approach based on a second derivative method [6] was used to calculate the activation energy. The first derivative of Eq. (5) was considered and it was assumed that $f(\alpha) = (1-\alpha)^n$, so

$$\frac{d}{dT}\left(\frac{d\alpha}{dT}\right) = \frac{A}{\beta}\left[\frac{d(f(\alpha))}{d\alpha} e^{-E_a/RT} \frac{d\alpha}{dT} + f(\alpha)\frac{E_a}{RT^2} e^{-E_a/RT}\right] \tag{7}$$

This derivative is zero at the inflexion point of a TGA curve or at the maximum of a DTG curve. Rearranging and combining with Eq. (5) gives the Kissinger equation:

$$\ln\left(\frac{\beta}{T_{max}^2}\right) = \ln\left(-\frac{d(f(\alpha))}{d\alpha}\right) + \ln\left(\frac{AR}{E_a}\right) - \frac{E_a}{RT_{max}} \tag{8}$$

The activation energy was calculated by plotting $\ln(\beta/T_{max}^2)$ against $1/T_{max}$ ($T_{max}$ is the temperature where the second derivative of $d\alpha/dT$ is equal to zero).

The reaction order was determined from the following equation [7]:

$$n = \frac{E^a(1-\alpha_{max})}{(d\alpha/dT)_{max} RT_{max}^2} \tag{9}$$

This equation shows that for a zero-order process the DTG curve reaches a maximum $(d\alpha/dT)_{max}$ when the extent of reaction at this point ($\alpha_{max}$) is equal to

unity. In other words the curve abruptly returns to the baseline after $T_{max}$.

*2.1.3. Model fitting method*

The following model fitting method [8] was used for the isothermal experiments:

$$g(\alpha) = kt \tag{10}$$

where $g(\alpha)$ is an integral mathematical expression related to the reaction mechanism, $g(\alpha) = d\alpha/f(\alpha)$.

Plotting $\ln[k(T)]$ against $1/T$ according to the Arrhenius equation gives the activation energy $E_a$ and pre-exponential factor $A$ from the slope and the intercept, respectively. If the decomposition observed involves sublimation or vaporisation, the kinetic mechanism should be a zero-order process [9]. The rate of mass loss of a sample under isothermal conditions should be constant providing that the free surface does not change [10,11] and the extent of reaction ($\alpha$) or the fraction sublimated or evaporated is equal to the product of time and the rate constant ($g(\alpha) = \alpha = kt$).

*2.1.4. Modulated thermogravimetric analysis*

MTGA was used to calculate the activation energy as a function of the extent of reaction. MTGA is based on a method proposed by Flynn in 1968 [12] and has been developed and patented by TA Instruments. In MTGA, the rate of weight loss follows a sinusoidal temperature modulation which is superimposed on the linear heating rate according to Eq. (4). The deconvolution of signal according to a discrete Fourier transformation allows to calculate the kinetic parameters such as activation energy ($E_a$) and pre-exponential factor ($A$) without any assumptions concerning the kinetic model [13]. The software calculates $E_a$ from the following equation:

$$E_a = \frac{R(T^2 - A'^2)L}{2A'} \tag{11}$$

where $E_a$, $R$ and $T$ have their usual meanings, $A'$ the temperature amplitude and $L$ is the logarithmic ratio between the maximum and minimum rates of process on the peaks and on the valleys of the $T = f(t)$ plot. MTGA gives the same information as the isoconversional non-isothermal method but from a single run.

*2.2. Thermodynamics*

*2.2.1. Sublimation and vaporisation processes*

The Langmuir equation [10] was used to study sublimation and vaporisation processes:

$$\frac{dm}{dt} = p\gamma\sqrt{\frac{M}{2\pi RT}} \tag{12}$$

where $dm/dt$ is the rate of mass loss per unit area, $p$ the vapour pressure, $M$ the molecular weight of the vapour and $\gamma$ is the vaporisation coefficient equal to unity for a material volatilising in a vacuum. If we rearrange Eq. (12) we obtain

$$p = K\nu \tag{13}$$

where $K = (2\pi R)^{1/2}/\gamma$ and $\nu = (T/M)^{1/2}(dm/dt)$. Price and Hawkins [9] have shown that $K$ is independent of the sample providing that the molecules are not associated in the vapour phase. The $K$-value can be determined by calibration with a substance of known vapour pressure. Therefore, the diagram of $p = f(T)$ of an unknown material can be constructed.

The enthalpy associated to the sublimation or vaporisation process can then be calculated from the Clausius Clapeyron equation:

$$\frac{d\ln p}{dT} = \frac{\Delta H}{RT^2} \tag{14}$$

where $\Delta H$ is the molar enthalpy of sublimation ($\Delta H_{sub}$) or vaporisation ($\Delta H_{vap}$). If it is supposed that molar enthalpy is constant over the studied temperature range, the Clausius Clapeyron equation may be written as

$$\ln p = C - \frac{\Delta H}{RT} \tag{15}$$

Combining Eqs. (13) and (15) gives

$$\ln\left(\frac{dm}{dt}\sqrt{\frac{T}{M}}\right) = C' - \frac{\Delta H}{RT} \tag{16}$$

where $C' = C - \ln K$.

Thus, the sublimation or vaporisation enthalpies can be calculated from the slope of $\ln(p)$ plotted against reciprocal absolute temperature.

Finally, once the sublimation and vaporisation enthalpies are known the melting enthalpy can be calculated.

*2.2.2. Melting enthalpy*

The phase equilibrium between solid, liquid and vapour states may be written as shown in the Hess cycle

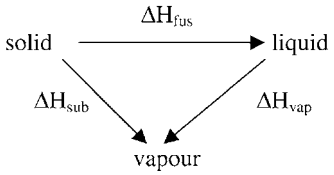


If the enthalpies are independent of the temperature between the melting and vaporisation temperatures, then $\Delta H_{sub} = \Delta H_{fus} + \Delta H_{vap}$, so

$$\Delta H_{fus} = \Delta H_{sub} - \Delta H_{vap} \quad (17)$$

*2.2.3. Solubility parameter*

Thermodynamic parameters such as the vaporisation enthalpy ($\Delta H_{vap}$) can be used to calculate the solubility parameter ($\delta$) [14,15] and predict the miscibility of a drug and a polymer in a formulation:

$$\delta = \sqrt{\frac{\Delta H_{vap} - RT}{V_m}} \quad (18)$$

where $V_m$ is the molar volume of the molecule.

Generally without favourable intermolecular interactions (e.g. hydrogen bonding) the molecular mixing between two substances is observed if the solubility parameters are very close.

## 3. Experimental

### 3.1. Materials

*S*(−) efaroxan, 2-[2-(2-ethyl-2,3-dihydro-2-benzofuranyl)]-imidazoline, CAS registry number [99197-32-0]. Its formula is $C_{13}H_{16}N_2O$:

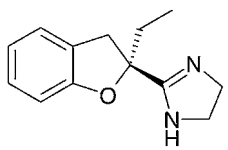


Efaroxan possesses an asymmetric carbon on the dihydrobenzofuranyl ring [C(2)] and therefore exhibits two enantiomers [16]. The resolution of *R* and *S* efaroxan hydrochloride was performed by preferential crystallisation in methanol after diastereoisomer salt formation with dibenzoyl tartaric acid. Chemical and optical purities were evaluated by HPLC and exceeded 99.5% w/w (internal normalisation). The sublimate was obtained from the initial powder maintained for several hours at 190 °C in a round-bottomed flask with magnetic stirring in an oil bath and surmounted by a water cooler. The sublimate was crystallised in the water cooler and collected by means of a spatula. Acetanilide was purchased from ThermoQuest (batch number 1318) and benzoic acid Merck (batch number 02401B), respectively. Chemical purities exceeded 99.5% w/w.

### 3.2. Methods

*3.2.1. High performance liquid chromatography*

Chemical purity was determined by HPLC on a Merck Hitachi Lachrom apparatus fitted with a symmetry C8 column, 5 μm, 250 mm × 4.6 mm (Waters) temperature maintained at 25 °C and mobile phase consisting of acetonitrile–water–$KH_2PO_4$ (150 ml/850 ml/6.8 g) adjusted to pH = 5.5. Optical purity was determined by HPLC using a Chiralcel OD column with hexane–ethanol–diethylamine (95 ml/5 ml/0.05 ml) as the mobile phase. Flow rate was set to 1 ml $min^{-1}$ and UV detection at 220 nm.

*3.2.2. Elemental analysis*

Elemental analyses to determine the carbon, hydrogen and nitrogen weight percentages were performed on a Fisons 1108 CHN elemental analyser. The instrument was calibrated with acetanilide as standard and BBOT (2,5-bis(5-*tert*-butyl-benzoxazol-2-yl) thiophen as a check point. Samples of approximately 1 mg were weighed on a Mettler ultramicrobalance UMT2.

*3.2.3. Fourier transform infrared spectroscopy*

FTIR spectrum was recorded on a Nicolet 510P Fourier transform spectrometer at a resolution of 2 $cm^{-1}$ in a wavenumber range from 400 to 4000 $cm^{-1}$ operated by Omnic software version 4.1b. Approximately 1 mg of sample was ground with about 130 mg of spectral quality KBr powder (Merck). The mixture was loaded into a cylindrical stainless steel die. The die was assembled and pressed at 10 t $cm^{-2}$. Spectra

were recorded with 32 scans and 4 $cm^{-1}$ resolution after treatment of data by Happ–Genzel function.

*3.2.4. Differential scanning calorimetry*

Differential scanning calorimetry (DSC) was performed on a DSC Q100 (TA Instruments) equipped with the Universal Analysis 2000 software. The instrument was calibrated (temperature and cell constant) using an indium standard (SPIN, Ref. LGC2601).

Assays were performed at the rate of 5 °C $min^{-1}$ in hermetically sealed aluminium pans from 0 to 260 °C under a nitrogen flow of 50 ml $min^{-1}$. Samples of about 3 mg were weighed on a Sartorius ultramicrobalance MP 8. The melting enthalpy and its uncertainty were expressed by the mean and standard deviation of three assays.

*3.2.5. Thermogravimetric analysis*

TGA and DTG curves were obtained using a TA High Resolution 2950 thermogravimeter analyser equipped with the Universal Analysis 2000 software (TA Instruments) and a nitrogen purge at 60 ml $min^{-1}$. The sample was weighed in an open aluminium crucible with a cross-sectional area of 0.327 $cm^2$ and deposited in a platinum pan. A sample of 5–9 mg was used to cover the whole of the crucible section uniformly. The thermobalance was calibrated for temperature by melting tin. The magnitude and linearity of the balance response were checked using standard milligram masses.

The non-isothermal TGA was recorded at several heating rates (1, 2, 3 and 5 °C $min^{-1}$) from room temperature to 350 °C. For the isothermal condition, the TGA furnace was rapidly heated to the required temperature (30 °C $min^{-1}$) and the sample was maintained at this temperature for 40 min.

MTGA experiments were performed using three linear heating rates (1, 2 and 5 °C $min^{-1}$) with a modulation amplitude of 5 °C and a period of 200 s. Kinetic analyses were performed by converting the weight loss derivative $dW/dT$ or $dW/dt$ into the derivative of the extent of reaction $d\alpha/dT$ or $d\alpha/dt$ from Eq. (19):

$$\frac{d\alpha}{dx} = \frac{1}{W_i - W_f}\frac{dW}{dx}, \quad x = T \text{ or } t \tag{19}$$

In fact, when activation energy is determined using differential methods it is independent of the signal derivative form since it was calculated from the slope of plots $\ln(\beta(d\alpha/dT))$ versus $1/T$ (Friedman method) or $\ln(\beta/T_{max}^2)$ against $1/T_{max}$ (Kissinger method). But the pre-exponential term ($A$) and the model ($f(\alpha)$) determined from the intercept of the linear regression depend on the signal derivative form. Therefore, the conversion, according to Eq. (19) was necessary.

The uncertainties of kinetic parameters values were expressed as standard deviations calculated by the least square method. The TGA experiments used to construct the curve $p = f(T)$ were performed at 5 °C $min^{-1}$.

## 4. Results and discussion

The TGA and DTG curves of $S(-)$ efaroxan hydrochloride (Fig. 1) show a weight loss without any residue at the end of the transition, the return of the DTG curve to the baseline is very steep almost perpendicular. This behaviour is compatible with a sublimation process. To confirm this, we isolated a few milligrams of the sublimate.

The samples were analysed by high performance liquid chromatography (HPLC) to evaluate its chemical and optical purities, by elemental analysis to know chemical composition, by Fourier transform infrared spectroscopy (FTIR) and by differential scanning calorimetry (DSC).

The FTIR spectrum of the initial powder are was identical to that of the sublimate, indicating that the chemical functions were unchanged by the thermal treatment. Six assays were performed to determine the chemical composition of the sublimate in carbon, hydrogen and nitrogen element. The means and standard deviations were calculated. The results are reported in Table 1 and show that the elemental composition in carbon, hydrogen and nitrogen was consistent with the theoretical value, confirming that the weight loss corresponds to a sublimation. Chemical and optical

Table 1
Elemental analysis result

| Element | Theoretical composition (% w/w) | Experimental composition (% w/w) | Uncertainty (2S.D.) |
|---|---|---|---|
| Carbon | 61.78 | 61.91 | ±0.12 |
| Hydrogen | 6.78 | 6.83 | ±0.10 |
| Nitrogen | 11.08 | 11.09 | ±0.16 |

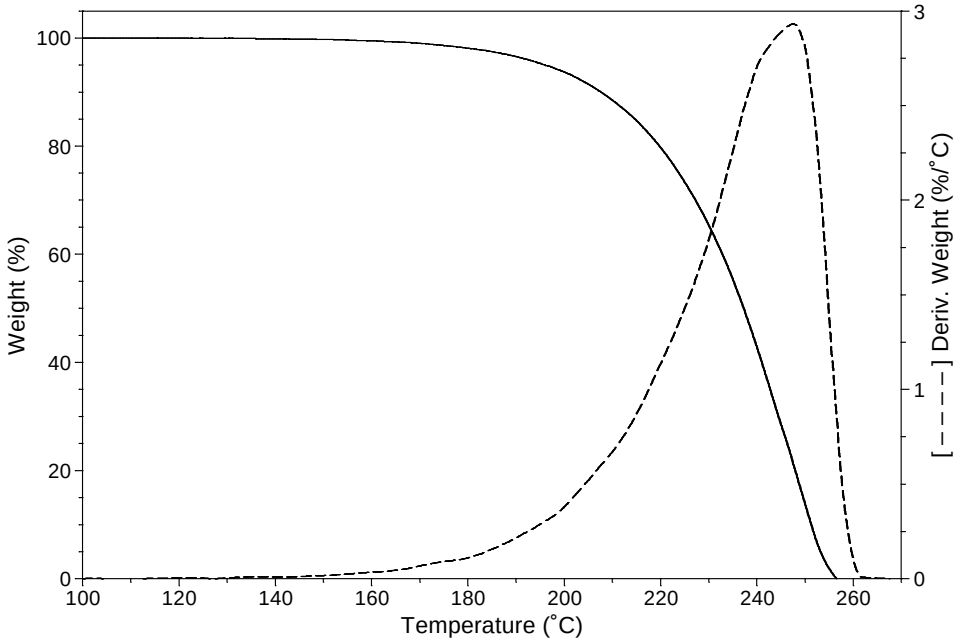


Fig. 1. TGA and DTG curves of *S*(−) efaroxan hydrochloride at 5 °C min$^{-1}$.

purities were greater than 99.5% w/w. The differential scanning calorimetry (DSC) of the sublimate (Fig. 2) showed a slight and broad endotherm starting at 192 °C with enthalpy of 3.17 kJ mol$^{-1}$ followed by melting at 245.5 °C. The initial powder showed only a single endotherm at 247.5 °C corresponding to melting, $\Delta H = 30.05 \pm 0.60$ kJ mol$^{-1}$. These DSC results suggest that the sublimate crystallised as a new polymorph.

### 4.1. Friedman method

DTG curves were used to perform the kinetic analysis based on the Friedman method. The relation between $\ln(\beta(\mathrm{d}\alpha/\mathrm{d}T))$ and $1/T$ was established using Eq. (6) with various values of $\alpha$ from 0.10 to 0.90 by steps of 0.05.

The differentiation was sensitive to noise in the experimental $\alpha/T$ curve and the data were smoothed. The side reaction $\alpha < 0.10$ and $\alpha > 0.90$ was not studied because the derivative signal was too low or too flat to be measured accurately.

The determination coefficients ($r^2$) exceeded 0.9780 indicating a good fit of experimental data by Eq. (6). Activation energies for each $\alpha$-value were determined from the slope of $\ln(\beta(\mathrm{d}\alpha/\mathrm{d}T))$ against $1/T$. Activation energy uncertainties were always less than 10.5% (relative standard deviation). The diagram of $E_a = f(\alpha)$ calculated by the Friedman method is shown in Fig. 3. It can be seen that the activation energy were rather constant over the whole range of $\alpha$, at $115 \pm 5$ kJ mol$^{-1}$. This result suggests with a single step a mechanism [17] in agreement with a sublimation process.

### 4.2. Kissinger method

The Kissinger method was used to calculate the activation energy, which was determined to be $113.6 \pm 3.4$ kJ mol$^{-1}$. The determination coefficient ($r^2$) of the plot of $\ln(\beta/T_{max}^2)$ against $1/T_{max}$ was 0.9983. The activation energy value determined by the Kissinger method agreed with that determined using the Friedman method.

### 4.3. Model fitting method

Investigation of the sublimation process was followed by isothermal experiments at 150, 155, 160, 165, 170, 175, 180, 185 and 190 °C. Fig. 4 shows the

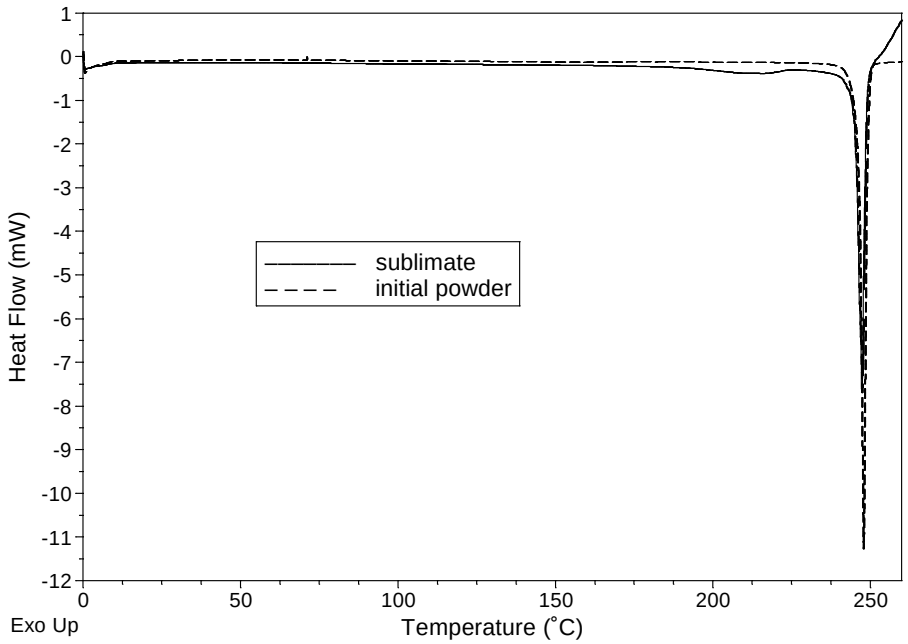


Fig. 2. DSC curves: (solid line) initial powder; (dashed line) sublimate crystal.

profile obtained by plotting weight loss and temperature against time. The initial weight percent ($W_i$) was recorded when the isotherm was reached (11 min). The values $W_t$ were used to calculate the extent of reaction ($\alpha$) and $\alpha$-time plots were constructed for each isotherm (Fig. 5).

Variations of $\alpha$ against time were linear and the slopes increased with the temperature. These results confirmed that the sublimation process followed a zero-order mechanism. The rate constant was determined both by linear regression of the $\alpha$-time plots and from isothermal runs since a zero-order mechanism gives $k = d\alpha/dt$.

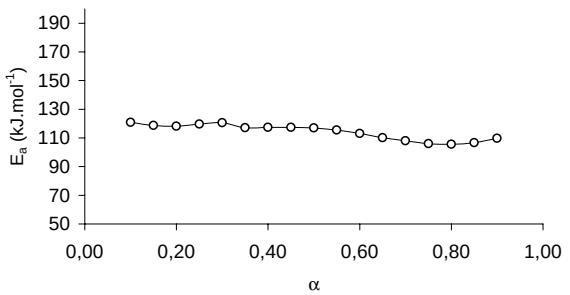


Fig. 3. Diagram of $E_a = f(\alpha)$.

The determination coefficients ($r^2$) of the linear regressions exceeded 0.9980.

The rate of mass loss ($d\alpha/dt$) was constant during the isothermal run but varied slightly over time at the high temperatures (190 °C). This phenomenon may be due to the changes sample surface and perhaps an increase in the partial pressure within the oven. The $d\alpha/dt$ value was therefore recorded after 30 min into the run. The results are reported in Table 2. Linear regression data were used to calculate the activation energy and the pre-exponential factor by applying the Arrhenius equation (3).

Table 2
Rate constants from isotherm runs

| $T$ (°C) | $k$ (min$^{-1}$) ($\alpha$-time plot) | S.D. (min$^{-1}$) | $k$ (min$^{-1}$) (DTG isotherm) |
|---|---|---|---|
| 150 | 0.000615 | 0.0000027 | 0.0006214 |
| 155 | 0.000962 | 0.0000059 | 0.0009573 |
| 160 | 0.001246 | 0.0000097 | 0.001255 |
| 165 | 0.001711 | 0.0000048 | 0.001693 |
| 170 | 0.002979 | 0.0000115 | 0.002905 |
| 175 | 0.003825 | 0.0000142 | 0.003736 |
| 180 | 0.004923 | 0.0000133 | 0.004801 |
| 185 | 0.007458 | 0.0000292 | 0.007290 |
| 190 | 0.010831 | 0.0000347 | 0.010510 |

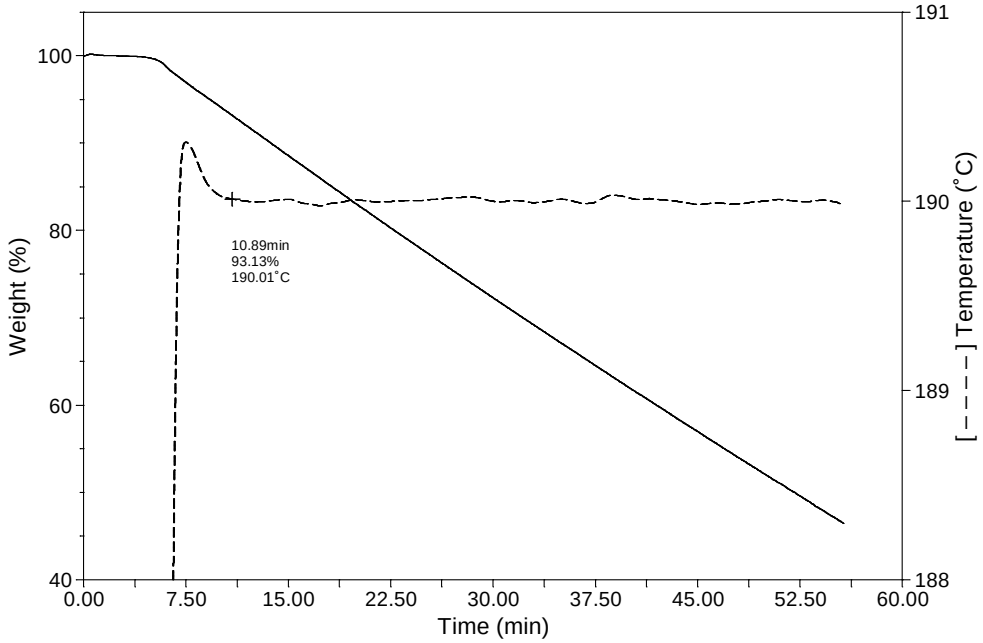


Fig. 4. Isotherm at 190 °C: profiles of weight loss and temperature against time.

The determination coefficient for the plot of ln($k$) against reciprocal absolute temperature was 0.9955, activation energy $E_a = 114.9 \pm 2.9\,\mathrm{kJ\,mol^{-1}}$ and the pre-exponential factor, $\ln A = 25.3 \pm 0.7$. It is interesting to note that the pre-exponential factor can be calculated from the non-isothermal method but here the kinetic model ($f(\alpha)$) is required since the intercepts of Eqs. (6) and (8) depend on these parameters.

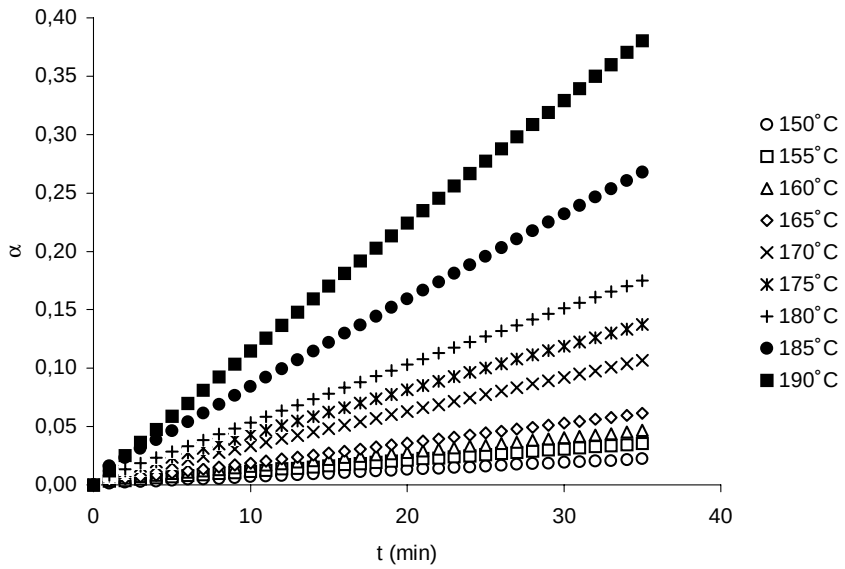


Fig. 5. The $\alpha$-time plots.

The intercepts correspond to $\ln A + \ln(f(\alpha))$ and $\ln(AR/E_a) + \ln[d(f(\alpha))/d\alpha]$ in the Friedman and Kissinger methods, respectively. The pre-exponential ($\ln A$) value was 22.8 and for the Kissinger method and between 22.5 and 26.7 for the Friedman method depending on the extent of reaction. The values of pre-exponential factor were very similar in both the methods and suggest that $f(\alpha) = 1$.

### 4.4. MTGA results

The MTGA was used to establish the relation between activation energy and the extent of reaction (Fig. 6). It was noted that $E_a$ values increased when as the heating rate decreased.

At the highest heating rate ($5\,^{\circ}C\,min^{-1}$) no flat plateau was obtained on the whole range of the extent of reaction. It is possible that insufficient periods were used to measure correctly the process activation energy. However, the profiles of $E_a = f(\alpha)$ at 1 and $2\,^{\circ}C\,min^{-1}$ are in good agreement with these obtained by the Friedman method.

Table 3
Sublimation enthalpies from plotting $\ln(\nu)$ against $1/T$ at 1, 2, 3 and $5\,^{\circ}C\,min^{-1}$

| $\beta$ ($^{\circ}C\,min^{-1}$) | $\Delta H_{sub}$ ($kJ\,mol^{-1}$) | S.D. ($kJ\,mol^{-1}$) |
|---|---|---|
| 1 | 99.13 | ±0.66 |
| 2 | 97.50 | ±0.43 |
| 3 | 96.76 | ±0.18 |
| 5 | 96.67 | ±0.19 |

### 4.5. Sublimation, vaporisation and melting enthalpies

Sublimation enthalpy was determined from the DTG curves of the non-isothermal runs at 1, 2, 3 and $5\,^{\circ}C\,min^{-1}$, the data points were taken on the rising range of the DTG curves. The results are reported in Table 3.

The determination coefficients ($r^2$) of plot $\ln(\nu) = f(1/T)$ were all greater than 0.9980 indicating a good correlation. It was observed that the value obtained for sublimation enthalpy was consistent with an endothermic process and decreased when the heating rate increased. The process is non-activated since

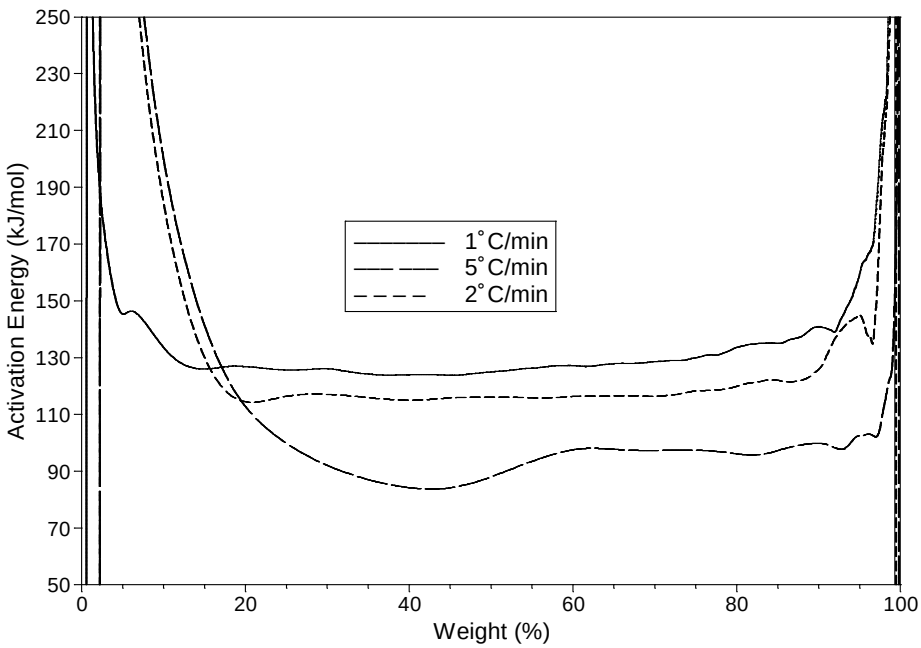


Fig. 6. $E_a$ calculated as a function of the extent of reaction ($\alpha$) using MTGA.

the sublimation enthalpy value is very similar to the activation energy.

In the isothermal experiments, we calculated sublimation enthalpy from the rate constant determined from the slope of the $\alpha$-time plots. The determination coefficient for the plot of $\ln(\nu) = f(1/T)$ was 0.9957. The sublimation enthalpy value was $116.8 \pm 2.9\,\mathrm{kJ\,mol^{-1}}$, higher than the values obtained from non-isothermal data.

The isothermal experiments were unsuitable for measuring the vaporisation enthalpy because the rates of weight loss were too fast. We preferred to use the non-isothermal experiments because it was possible to shift the weight loss process after the *S*(−) efaroxan hydrochloride melting point (245 °C) and thus measure the liquid to vapour phase transition.

The heating rate of $20\,^{\circ}\mathrm{C\,min^{-1}}$ produced a sufficient shift in the DTG curve since we observe the melting disturbance at 242.6 °C (Fig. 7). The temperature range (260–284 °C) was selected to collect the data in order to ensure that the vaporisation process is occurring from a constant liquid interface.

In order to determine the thermodynamic parameters of the melting process, we measured sublimation enthalpy from the same DTG plot between 200 and 240 °C. The plots of $\ln(\nu)$ against $1/T$ are shown in Fig. 8.

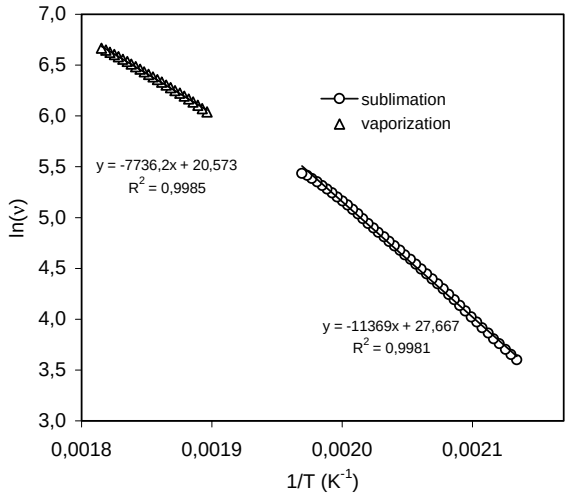


Fig. 8. Plot of $\ln(\nu)$ against reciprocal of absolute temperature.

The sublimation and vaporisation enthalpies calculated from the slopes correspond to $94.5 \pm 0.7$ and

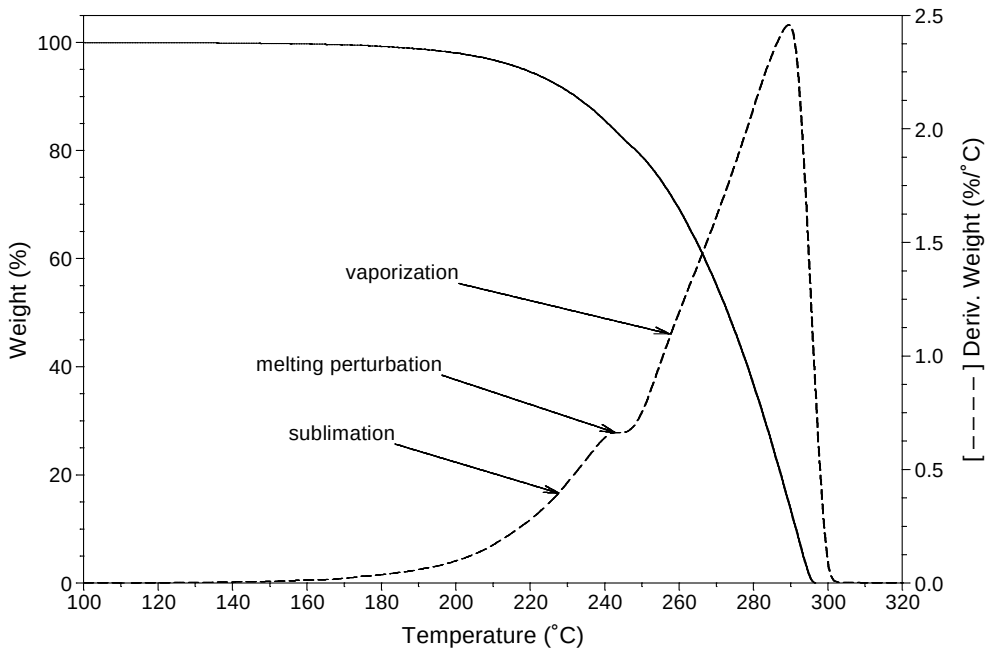


Fig. 7. DTG curves showing the melting perturbation.

$64.3 \pm 0.5\,\mathrm{kJ\,mol^{-1}}$, respectively. The sublimation enthalpy is greater than the vaporisation enthalpy by $30.2 \pm 1.2\,\mathrm{kJ\,mol^{-1}}$, in very good agreement with the melting enthalpy measured by DSC. We consider that vaporisation enthalpy was underestimated in these experimental conditions since the sublimation enthalpy value depends on the heating rate and we believe that vaporisation enthalpy varies in the same manner. We calculated the vaporisation enthalpy again using sublimation enthalpy data determined from the isothermal run ($116.8\,\mathrm{kJ\,mol^{-1}}$) and Eq. (17), so $\Delta H_{\mathrm{vap}} = 86.6 \pm 4.1\,\mathrm{kJ\,mol^{-1}}$.

### 4.6. Solubility parameter

The value determined for vaporisation enthalpy allowed us to calculate solubility parameters at 25 °C using Eq. (18). Without knowing the heat capacity of the liquid and vapour phases, it is difficult to evaluate the vaporisation enthalpy at 25 °C. Chickos et al. [18] suggest a method to calculate the vaporisation enthalpy as a function of temperature based on studies of a wide range of materials:

$$\Delta H_{\mathrm{vap}}(298\,\mathrm{K}) = \Delta H_{\mathrm{vap}}(T) + 0.0540(T - 298) \tag{20}$$

where $\Delta H_{\mathrm{vap}}$ is expressed in $\mathrm{kJ\,mol^{-1}}$ and $T$ is the temperature ($K$) at which the measurement is made (518 K). So, $\Delta H_{\mathrm{vap}}(298\,\mathrm{K}) = 98.5\,\mathrm{kJ\,mol^{-1}}$.

The molecular volume ($V_{\mathrm{m}}$) was estimated from crystallographic data [16] considering two molecules in an asymmetric unit, $V_{\mathrm{m}} = 195\,\mathrm{cm^3\,mol^{-1}}$. The uncertainty of the solubility parameter ($u(\delta)$) was calculated [19] from the relative uncertainties of the vaporisation enthalpy ($u(\Delta H_{\mathrm{vap}})/\Delta H_{\mathrm{vap}}$) and molecular volume ($u(V_{\mathrm{m}})/V_{\mathrm{m}}$) corresponding to 0.05 (5%) and 0.005, respectively

$$u(\delta)^2 = \delta^2 \left[ \frac{1}{2} \left( \frac{u(\Delta H_{\mathrm{vap}})}{\Delta H_{\mathrm{vap}}} \right)^2 + \frac{1}{2} \left( \frac{u(V_{\mathrm{m}})}{V_{\mathrm{m}}} \right)^2 \right] \tag{21}$$

So, $\delta = 10.85 \pm 0.40\,(\mathrm{cal\,cm^{-3}})^{0.5}$.

### 4.7. Vapour pressure

The vapour pressure of $S(-)$ efaroxan hydrochloride sublimation was established using acetanilide as the calibration compound. The vapour pressure of acetanilide as a function of temperature was obtained from the data published in the Handbook of Vapour Pressure [20].

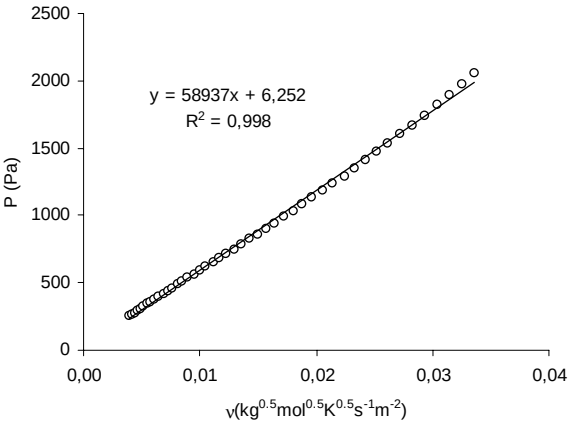


Fig. 9. The linear relationship between $p$ and $\nu$ of acetanilide.

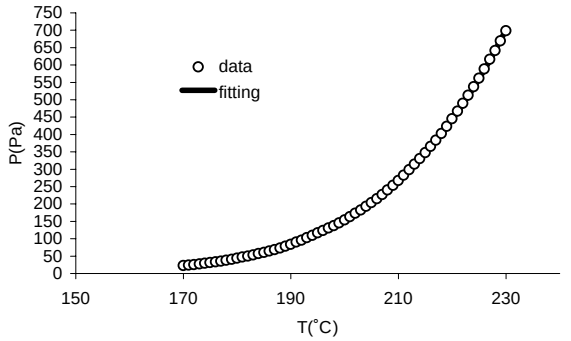


Fig. 10. Diagram of $p = f(T)$ of sublimation process.

The plot of $p$ against $\nu$ (Fig. 9), is linear ($r^2 = 0.9980$) and the value for $K$ was found to be $58\,937 \pm 397\,\mathrm{Pa\,s\,m^2\,kg^{-1/2}\,mol^{-1/2}\,K^{-1/2}}$. This value was confirmed using benzoic acid [21] as a second calibration substance, $K = 60\,561 \pm 663\,\mathrm{Pa\,s\,m^2\,kg^{-1/2}\,mol^{-1/2}\,K^{-1/2}}$ and $r^2 = 0.9955$. The vaporisation enthalpy of benzoic acid was $63.3 \pm 0.6\,\mathrm{kJ\,mol^{-1}}$ between 401 and 416 K, in excellent agreement with literature data [9], 66–69 $\mathrm{kJ\,mol^{-1}}$.

The data were taken on the rising range of the DTG between 170 and 230 °C and we plotted the diagram of $p = f(T)$ for $S(-)$ efaroxan hydrochloride (Fig. 10) using the $K$-value. The data were fitted with

Table 4
Fitting results from Antoine equation

| | Parameters | | |
|---|---|---|---|
| | *a* | *b* | *c* |
| Values | 7.348 | 1061.110 | 267.282 |
| S.D. | 0.078 | 33.833 | 3.466 |
| $r^2$ | 0.99996 | | |
| S.E. | 1.21899 | | |

the Antoine equation (22):

$$\log(p) = A - \frac{B}{C + T} \tag{22}$$

where $p$ is the pressure (Pa), $A$, $B$ and $C$ are the Antoine constants and $T$ is the temperature (K).

The fit was made by minimising the sum of residual squares (SRQ) between the experimental data $(\log(p)_{exp})$ and the calculated values $(\log(p)_{cal})$, $[\log(p)_{exp} - \log(p)_{cal}]^2$. The results are reported in Table 4.

## 5. Conclusion

We showed that *S*(−) efaroxan hydrochloride, and consequently *R*(+) enantiomer sublimate by a zero-order mechanism. The physicochemical analysis of the sublimate by HPLC, FTIR spectroscopy and elemental analysis showed that the chirality and chemical composition of molecule are unchanged, but the DSC analysis suggested that the sublimate crystallised as a new polymorph. The kinetic parameters were determined by non-isothermal, isothermal TGA and MTGA.

Sublimation enthalpy was similar to the activation energy, suggesting a non-activated process. The vaporisation enthalpy was also determined and used to calculate the solubility parameter, which is often employed to predict the drug–polymer miscibility in the pharmaceutical industry. The melting enthalpy calculated from the difference between $\Delta H_{sub}$ and $\Delta H_{vap}$ was consistent with the value obtained by DSC.

Finally, the pressure–temperature diagram of the sublimation was constructed from the Langmuir equation using acetanilide and benzoic acid as calibration substances. The fitting of vapour pressure was performed with the Antoine equation using a least square method.

## Acknowledgements

The authors wish to thank Dr. Mark S. Kleven for his assistance in the preparation of this manuscript.

## References

[1] S. Tellez, F. Colpaert, M. Marien, Eur. J. Pharmacol. 277 (1995) 113.
[2] R. Pena, A. Chauvet, J. Masse, J.P. Ribet, J.L. Maurel, J. Therm. Anal. 53 (1998) 123.
[3] R. Pena, A. Chauvet, J. Masse, J.P. Ribet, J.L. Maurel, J. Therm. Anal. 53 (1998) 697.
[4] U.J. Griesser, M. Szelagiewicz, U. Ch. Hofmeier, C. Pitt, S. Cianferani, J. Therm. Anal. Cal. 57 (1999) 45–60.
[5] R.R. Keuleers, J.F. Janssens, H.O. Desseyn, Thermochim. Acta 385 (2002) 127.
[6] D. Chen, X. Gao, D. Dollimore, Thermochim. Acta 215 (1993) 109.
[7] M.E. Brown, Handbook of Thermal Analysis and Calorimetry: Principles and Practice, vol. 1, Elsevier, Amsterdam, 1998.
[8] A.K. Galwey, M.E. Brown, Thermochim. Acta 269–270 (1995) 1.
[9] D.M. Price, M. Hawkins, Thermochim. Acta 315 (1998) 19.
[10] S.J. Ashcroft, Thermochim. Acta 2 (1971) 512.
[11] D.M. Price, J. Therm. Anal. Cal. 64 (2001) 315.
[12] J.H. Flynn, in: R.F. Schwenker, P.D. Garn (Eds.), Thermal Analysis, vol. 2, Academic Press, Budapest, 1969.
[13] R.L. Blaine, B.K. Hahn, J. Therm. Anal. Cal. 54 (1998) 695.
[14] M.M. Coleman, J.F. Graf, P.C. Painter, Specific Interactions and the Miscibility of Polymer Blends: Practical Guides for Predicting & Designing Miscible Polymer Mixtures, Technomic Publishing Co., Lancaster, 1991.
[15] J.I. Wells, Pharmaceutical Preformulation: The Physicochemical Properties of Drug Substances, Halsted Press, 1988.
[16] C. Belin, A. Chauvet, J.M. Leloup, J.P. Ribet, J. L Maurel, Acta Cryst. C 51 (1995) 2439.
[17] S.V. Vyazovkin, A.I. Lesnikovich, Thermochim. Acta 165 (1990) 273.
[18] J.S. Chickos, S. Hosseini, D.G. Hesse, J.F. Liebman, Struct. Chem. 4 (1993) 271.
[19] Quantifying uncertainty in analytical measurement, in: EURACHEM/CITAC Guide, 2nd ed., 2000.
[20] C.L. Yaws, Handbook of Vapor Pressure, vol. 3, Gulf Publishing Company, Texas, 1994.
[21] G. Hakvoort, C.M. Hol, P.J. van Ekeren, J. Therm. Anal. Calc. 69 (2002) 333.